Available online at www.sciencedirect.com
SCIENCE DIRECT
Journal of Power Sources 158 (2006) 641–645
JOURNAL OF POWER SOURCES
www.elsevier.com/locate/jpowsour

Short communication

Effect of (Al, Mg) substitution in $LiNiO_2$ electrode for lithium batteries

J. Kim [a,*], B.H. Kim [a], Y.H. Baik [a], P.K. Chang [a], H.S. Park [a], K. Amine [b]

[a] *Department of Materials Science and Engineering, Chonnam National University, 300 Yongbongdong, Bukku, Gwanju 500-757, South Korea*
[b] *Chemical Engineering Division, Argonne National Laboratory, 9700 South Cass Ave., Argonne, IL 60439, USA*

Received 11 May 2005; accepted 5 August 2005
Available online 19 October 2005

Abstract

Stabilized lithium nickelate is receiving increased attention as a low-cost alternative to the $LiCoO_2$ cathode now used in rechargeable lithium batteries. Layered $LiNi_{1-x-y}M_xM_yO_2$ samples ($M_x = Al^{3+}$ and $M_y = Mg^{2+}$, where $x = 0.05$, 0.10 and $y = 0.02$, 0.05) are prepared by the refluxing method using acetic acid at 750 °C under an oxygen stream, and are subsequently subjected to powder X-ray diffraction analysis and coin-cell tests. The co-doped $LiNi_{1-x-y}Al_xMg_yO_2$ samples show good structural stability and electrochemical performance. The $LiNiAl_{0.05}Mg_{0.05}O_2$, cathode material exhibits a reversible capacity of 180 mA h g^{-1} after extended cycling. These results suggest that the threshold concentration for aluminum and magnesium substitution is of the order of 5%. The co-substitution of magnesium and aluminium into lithium nickelate is considered to yield a promising cathode material.

Keywords: Lithium batteries; Lithium nickelate; Layered compound; Aluminium and magnesium co-substitution; Refluxing method

1. Introduction

Although $LiCoO_2$ is the predominant cathode material used in lithium batteries at present, its high cost and toxicity have led to much enormous interest in developing alternative cathode materials. Both $LiNiO_2$ [1] and $LiMn_2O_4$ [2,3] are quite attractive materials in this regard. Layered $LiNiO_2$ has a stronger potential for high rate and high power applications, because its two-dimensional layered structure endows it with better lithium ionic and electronic conductivities than three-dimensional spinel $LiMn_2O_4$. In contrast to $LiCoO_2$, which has the same structure, it is very difficult to obtain phase pure and ordered $LiNiO_2$ because of the reduction of Ni^{3+} to Ni^{2+} that occurs at higher temperatures [4,5]. Furthermore, the migration of Ni^{2+} to the lithium plane results in disordered non-stoichiometric $Li_{1-x}Ni_{1+x}O_{2-z}$ and degrades its electrochemical performance. Accordingly, several attempts have been made to stabilize the $LiNiO_2$ structure. To date, the partial substitution of Co^{3+} for Ni^{3+} to give $LiNi_{1-x}Co_xO_2$ has been shown to produce attractive electrochemical properties and has become the most common approach [6]. Nevertheless, the cost and environmental concern associated with the use of Co^{3+} means that the search continues for less expensive and environmentally benign materials. Also, safety concerns regarding the abrupt exothermic reaction of charged $LiNiO_2$ continues to pose a problem, even after cobalt substitution. Substitution with other metals such as Al, Mn, Fe, Nb, etc., has been examined as a means to enhance the electrochemical performance of the cathode [7–9].

This papers presents a new substitution method using Al^{3+} and Mg^{2+} ions in order to stabilize the structure of the $LiNiO_2$ and enhance its performance. In this substitution, Al^{3+} and Mg^{2+} ions partially replace the Ni^{3+} ions in the $LiNi_{1-x-y}Al_xMg_yO_2$ phases with ranges of $x = 0.05$, 0.10 and $y = 0.02$, 0.05. The Al^{3+} and Mg^{2+} ions serve to improve the thermal and electrical properties, respectively. A refluxing method employing acetic acid was used for the preparation of the new compound, $LiNi_{1-x-y}Al_xMg_yO_2$.

2. Experimental

Appropriate amounts of lithium, aluminum, magnesium and nickel acetates were dissolved in de-ionized water to produce a stoichiometric mixture. An appropriate amount of acetic acid was then added to this solution. Here, acetic acid plays the role of a chelating agent. The solution was refluxed in a round-bottom

* Corresponding author. Tel.: +82 62 530 1703; fax: +82 62 530 1699.
E-mail address: jaekook@chonnam.ac.kr (J. Kim).

0378-7753/$ – see front matter © 2005 Elsevier B.V. All rights reserved.
doi:10.1016/j.jpowsour.2005.08.028

flask attached to a condenser at 80 °C for about 2 h. The clear solution was then evaporated and dried to yield the gel precursor. In order to eliminate the organic contents, the gel precursor was calcined at 400 °C for 1 h. The resulting black powder was ground well and heated at 750 °C for 30 h in oxygen atmosphere. The crystalline nature of the $LiNi_{1-x-y}Al_xMg_yO_2$ samples was confirmed by X-ray diffraction phase analysis. The morphology of the particles was observed by means of scanning electron microscopy (SEM).

The electrochemical performance of the $LiNi_{1-x-y}Al_xMg_yO_2$ electrodes was determined by conducting galvanostatic cycling experiments. Coin-type cells with the different cathode materials were prepared inside an argon-filled grove box. The electrolyte consisted of 1 M $LiPF_6$ with ethylene carbonate and diethyl carbonate (1:1 ratio). The $LiNi_{1-x-y}Al_xMg_yO_2$ powders were mixed with 10 wt.% carbon and 10 wt.% PVDF binder in 1-methyl-2-pyrrodinone solvent. The resulting paste was cast on an aluminum foil. The working electrodes each had a geometric area of 1.6 cm^2. The cells between 4.3 and 2.8 V at a current density of 0.2 mA cm^{-2}.

The area specific impedance (ASI) values were investigated by the HPPC (hybrid pulse power characteristic) testing method [10], in order to determine the dynamic power capability over the battery's useable charge and voltage range. The test profile incorporated both discharge and regenerative pulses. After establishing both the V_{min} cell discharge power capability at the end of an 18-s discharge current pulse and the V_{max} cell regenerative power capability over the first 2 s of a trapezoidal regenerative current pulse, the cell impedance and cell polarization impedance were calculated as a function of time. At first, the cell was charged at the *C*/1 rate to 4.1 V. After a 1-h rest, the cell was discharged to 10% depth-of-discharge (DoD) at the *C*/1 rate and then rested for another hour. This was followed by a series of partial (but increasing) *C*/1 discharges at 10% DoD increments, each of which was followed by an 18-s pulse discharge and a 2-s pulse charge at a very high rate (10–15 C). The ASI values were then calculated for both the 18-s pulse discharge and the 2-s pulse charge at each DoD.

3. Results and discussion

3.1. Morphology

A scanning electron micrograph of the $LiNi_{0.9}Al_{0.05}Mg_{0.05}O_2$ sample, which is representative of $LiNi_{1-x-y}Al_xMg_yO_2$ system, is presented in Fig. 1. The size of the $LiNi_{0.9}Al_{0.05}Mg_{0.05}O_2$ particles was examined since this parameter determines the effective surface area, and a smaller particle size improves the capacity of the battery by reducing the ion diffusion pathway during the Li^+ intercalation and de-intercalation processes [12]. The powders are found to consist of particles of sub-micron size, i.e., the average size of the agglomerated secondary particles was of the order of 5 μm. This unique morphology is advantageous for electrode materials, because it allows the electrochemical performance to be improved. On the other hand, the relatively large surface area that results from such a fine particle size might result in unfavourable safety features.

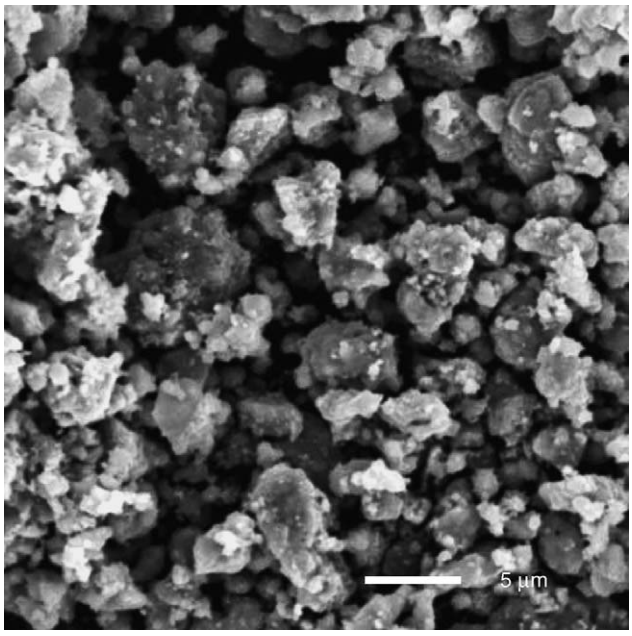

Fig. 1. Scanning electron micrograph of $LiNi_{0.9}Al_{0.05}Mg_{0.05}O_2$ sample.

3.2. Structural characterization

The X-ray diffraction (XRD) patterns of the $LiNi_{1-x-y}Al_xMg_yO_2$ compounds obtained using Cu Kα radiation are given in Fig. 2. The patterns show that the samples have phase-pure, layered structures. A single phase $LiNi_{1-x-y}Al_xMg_yO_2$, (where $x = 0.05$, 0.10 and $y = 0.02$, 0.05) with an α-$NaFeO_2$ type structure is grown when the precursors are fired at 750 °C in an oxygen

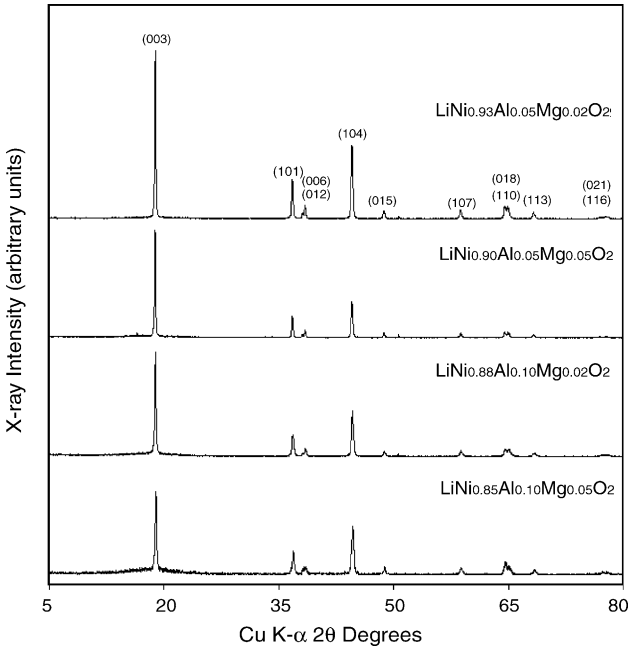

Fig. 2. X-ray diffraction patterns for $LiNi_{1-x-y}Al_xMg_yO_2$ compounds.

Table 1
Lattice parameters and trigonal distortion ratios of $LiNi_{1-x-y}Al_xMg_yO_2$ compounds

Compounds	Lattice parameter (Å)		Trigonal distortion c/a
	a	c	
$LiNi_{0.93}Al_{0.05}Mg_{0.02}O_2$	2.8736	14.1327	4.9181
$LiNi_{0.90}Al_{0.05}Mg_{0.05}O_2$	2.8728	14.1297	4.9184
$LiNi_{0.88}Al_{0.10}Mg_{0.02}O_2$	2.8716	14.1018	4.9107
$LiNi_{0.85}Al_{0.10}Mg_{0.05}O_2$	2.8721	14.0984	4.9087

atmosphere for 30 h. The XRD peaks were indexed to R-3 m symmetry.

Compared with samples that contain large amounts of aluminium and magnesium, those doped with lesser amounts of aluminum and magnesium have a very high Bragg intensity ratio $R_{(0\,0\,3)} = I_{(0\,0\,3)}/I_{(1\,0\,4)}$, which can serve as a measure of the stoichiometry and degree of order in the $LiNiO_2$ system. As the amount of Al and Mg concentration is increased, the Bragg intensity ratio is decreased, which suggests that the amounts of the co-dopants, aluminum and magnesium, should be kept at around 10%, in order to obtain a well-ordered layered structure.

The overall high intensity ratio of the (0 0 3) and (1 0 4) peaks and the clear splitting of the (0 1 8) and (1 1 0) peaks indicate that the $LiNi_{1-x-y}Al_xMg_yO_2$ compounds have good structural stability, without the presence of cobalt that is normally used to stabilize the $LiNiO_2$ phase. In this regard, the cobalt-free $LiNi_{1-x-y}Al_xMg_yO_2$ compounds represent particularly attractive alternatives in the quest for less expensive and less toxic materials.

The values of the lattice parameters were obtained from the XRD profiles using the unit cell program. The lattice parameters are listed in Table 1. As the amount of aluminum and magnesium in the $LiNi_{1-x-y}Al_xMg_yO_2$ samples increases, the average metal–metal intrasheet distance (a_{hex}) slightly decreases. In general, the average metal–metal interlayer distance ($c_{hex}/3$) also decreases. This is due to the formation of a relatively weak electrical repulsion between the layers due to the substitution by Mg^{2+} of a lower valency [11]. The Mg^{2+} ions appear to have different local ionic ordering compared with the Ni^{3+} ions, and tend to form less ionic $(Ni_{1-x-y}Al_xMg_yO_2)_n$ sheets, which yield lower *c*/*a* values. As a result, the lattice parameter along the *c*-axis decreases from 14.1327 to 14.0984 Å as the amount of the substituents increases, and a slight change in the *a*-value is also observed. This may also be due to the partial substitution of magnesium ions for aluminium in the lithium nickelate and to the ionic character of the Al–O bond [13]. Therefore, the overall *c*/*a* values of 4.92–4.91, which reflect the degree of trigonal distortion, are relatively low.

3.3. Electrical conductivity

Electrical conductivity measurements were performed using the d.c. four-probe technique. The results are summarized in Table 2. Samples with higher aluminum contents show lower conductivity, whereas Samples with higher magnesium contents have higher conductivity. This means that the presence of aluminum deteriorates the electrical conductivity, while that of magnesium improves it. Thus, careful optimization of both the ratio of aluminum to magnesium, and the ratio of aluminum and magnesium to nickel is required. Although there is no indication of the two-order increase in the magnitude of the electrical conductivity that occurs when 5% magnesium is substituted into $LiCoO_2$, some enhancement of the conductivity in the layered compound is obtained by forming a mixed valence state with the same amount (5%) of magnesium substitution. The overall values of the conductivity are sufficiently high for the $LiNi_{1-x-y}Al_xMg_yO_2$ to be considered as a promising electrode material for high-power applications.

Table 2
Electrical conductivities of $LiNi_{1-x-y}Al_xMg_yO_2$ compounds

Compound	Conductivity ($\times 10^3$ S m^{-1})
$LiNi_{0.93}Al_{0.05}Mg_{0.02}O_2$	1.73
$LiNi_{0.90}Al_{0.05}Mg_{0.05}O_2$	8.25
$LiNi_{0.88}Al_{0.10}Mg_{0.02}O_2$	0.72
$LiNi_{0.85}Al_{0.10}Mg_{0.05}O_2$	0.84

3.4. Electrochemical properties

The electrochemical performance of the $LiNi_{1-x}Al_xMgO_2$ ($x = 0.05$, 0.10 and $y = 0.02$, 0.05)/$LiPF_6$ in EC/DEC/Li cells on cycling at a current density of 0.2 mA cm^{-2} is shown in Fig. 3. The capacity decreases as the aluminum content increases, which is to be expected given that aluminum is not electrochemically active. Although aluminum substitution favours and maintains a layered structure by forming a $LiNi_{1-x}Al_xO_2$ solid solution with the same structure (R-3 m) as $LiNiO_2$ and α-$LiAlO_2$, the local distortion [15] of aluminum caused by the movement along the trigonal symmetric axis causes this material to lose its preferred occupation of 3a octahedral sites and leads to partial pseudo-tetrahedral coordination. Also, it is suspected that the formation of an aluminum-rich insulating phase in the fully-charged state (for example, $Li_{0.1}Ni_{1-x}Al_xO_2$)

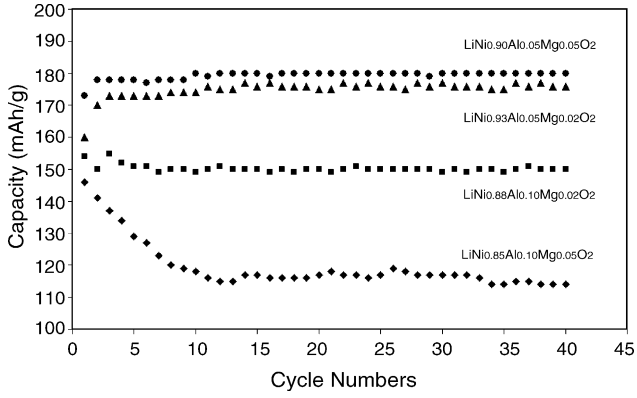

Fig. 3. Cycleabilities of $LiNi_{1-x-y}Al_xMg_yO_2$ compounds denoted by (▲) $LiNi_{0.93}Al_{0.05}Mg_{0.02}O_2$, (●) $LiNi_{0.90}Al_{0.05}Mg_{0.05}O_2$, (■) $LiNi_{0.88}Al_{0.10}Mg_{0.02}O_2$, (♦) $LiNi_{0.85}Al_{0.10}Mg_{0.05}O_2$.

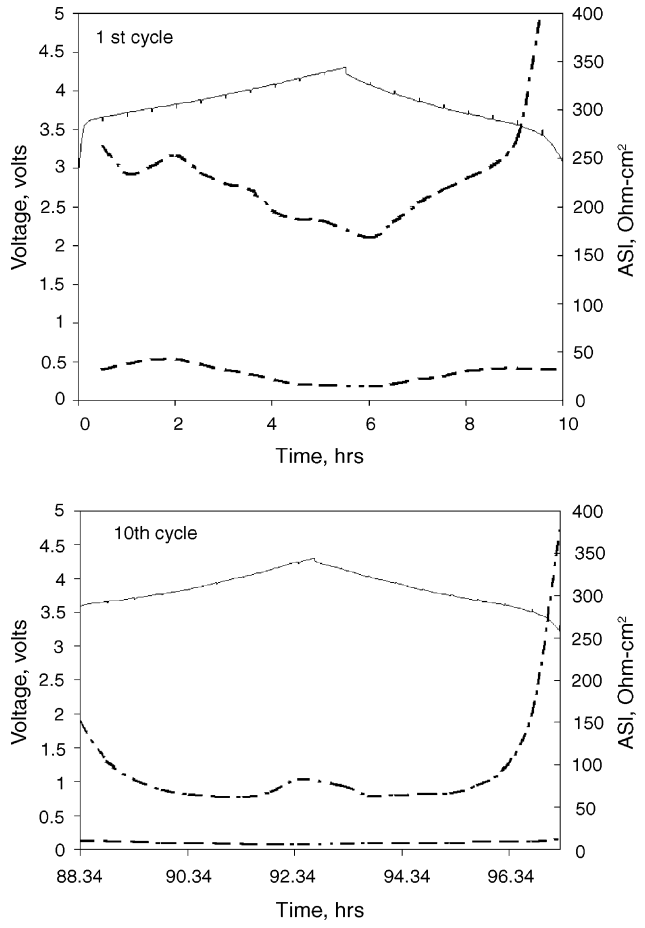

Fig. 4. Comparison of first and tenth area specific impedance (ASI) values of $LiNi_{0.90}Al_{0.05}Mg_{0.05}O_2$ electrode.

might harm the charge–discharge reversibility, although it is in fact beneficial from the point of view of overcharge protection. As expected, the electrodes with >10% aluminum had poor capacity retention. When magnesium is co-doped with aluminum in equal amounts, the capacity retention is increased. These results indicate that the threshold concentration for aluminum and magnesium substitution is of the order of 5%.

The $LiNi_{0.9}Al_{0.05}Mg_{0.05}O_2$, cathode material is found to exhibit a reversible capacity of 173 mA h g^{-1} on the first discharge cycle and this value increases with cycling, as shown in Fig. 3. It has been reported that the discharge capacity of $LiNi_{0.80}Co_{0.15}Al_{0.05}O_2$ is around 160 mA h g^{-1} [14], but decreases on cycling. The co-doped electrode, $LiNi_{0.90}Al_{0.05}Mg_{0.05}O_2$, exhibits a good reversible capacity with excellent capacity retention. This may be due to its particle size, morphology, etc., as well as to its good electrical conductivity and structural stability compared with the other samples with different concentrations of substituents.

The first and tenth charge–discharge curves of the $LiNi_{0.90}Al_{0.05}Mg_{0.05}O_2$ electrode, together with the corresponding ASI values, are presented in Fig. 4. The ASI values have distinctly decreased by the 10th cycle, which presents a higher capacity than in the initial cycling stage. This suggests

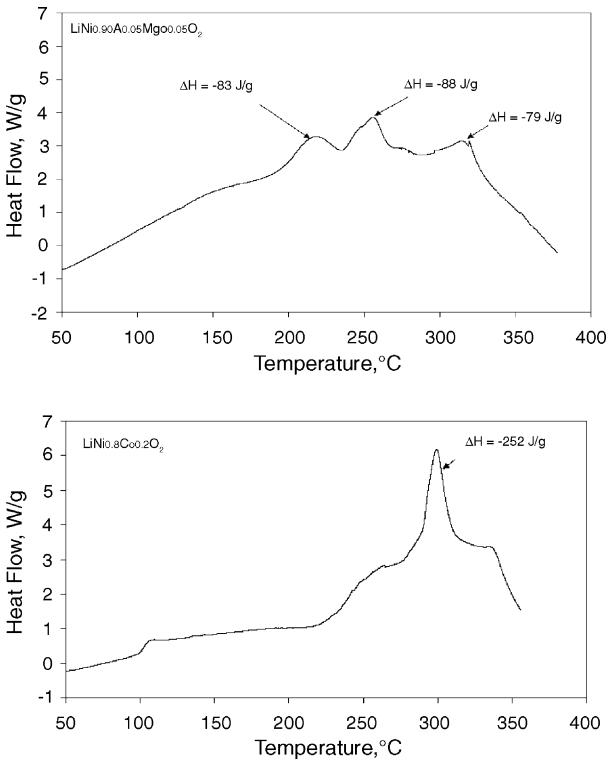

Fig. 5. Comparison of differential scanning calorimetry (DSC) plots of $LiNi_{0.90}Al_{0.05}Mg_{0.05}O_2$ and $LiNi_{0.80}Co_{0.20}O_2$ electrodes prepared from fully-charged state with fresh electrolyte.

that the $LiNi_{0.90}Al_{0.05}Mg_{0.05}O_2$ electrode has maintain its structural integrity during the cycling experiment. The observed high electrical conductivity of 8.25×10^{-3} S m^{-1} is believed to play a critical role in endowing this electrode with stable electrochemical performance, with the rigid framework of the layered structure also making some contribution.

Results obtained using the differential scanning calorimetry (DSC) technique, which allows the safety characteristics of electrode materials to be determined, show a discernible exothermic peak at a relatively low temperature of around 220 °C for $LiNi_{0.90}Al_{0.05}Mg_{0.05}O_2$. This may be due to the fine particle characteristics, as shown in Fig. 1. Compared with data obtained for commercially available $LiNi_{0.80}Co_{0.20}O_2$, the overall exothermic calorific values are similar, since aluminum helps to form a thermally stable structure, although the initial reaction occurs at an earlier stage (Fig. 5).

4. Conclusions

Compound of the general formula $LiNi_{1-x-y}M_xM_yO_2$ ($M_x = Al^{3+}$and $M_y = Mg^{2+}$, where $x = 0.05$, 0.10 and $y = 0.02$, 0.05) have been synthesized and evaluated as alternative cathode materials for lithium batteries. The electrodes are characterized by means of morphological and structural studies. Analysis with XRD shows that the prepared $LiNi_{1-x-y}M_xM_yO_2$ forms a single phase with good crystallinity. The XRD data also demonstrate that an ordered layered structure was successfully formed, without any cobalt being added. From the conductivity results, it is clear that deterioration of the conductivity

is alleviated by the co-substitution of magnesium at a concentration of 5%. The optimized ratio of aluminum and magnesium to nickel is found to be 5%. Among these prepared electrodes, $LiNi_{0.90}Al_{0.05}Mg_{0.05}O_2$ attains the highest reversible capacity, viz., 175 mA h g^{-1}, is and it also exhibits the lowest resistivity. Enhancement of the capacity retention is greater in the Mg co-doped lithium aluminium nickelate than in the undoped and Al-doped lithium nickelate. This suggests that the doping of magnesium reduces the phase transitions and maintains the layered structure. It is concluded that these cobalt-free $LiNi_{1-x-y}Al_xMg_yO_2$ compounds after promise as less expensive and less toxic materials for rechargeable lithium batteries.

Acknowledgements

The research was supported by the Program for the Training of Graduate Students in Regional Innovation that was conducted by the Ministry of Commerce, Industry and Energy of the Korean Government.

References

[1] W. Ebner, D. Fouchard, L. Xie, Solid State Ionics 69 (1994) 238.
[2] J.M. Tarascon, E. Wang, F.K. Shokoohi, W.R. Mekinnon, S. Colsons, J. Electrochem. Soc. 38 (1991) 2859.
[3] T. Ohzuku, M. Kitagawa, T. Hirai, J. Electrochem. Soc. 137 (1990) 769.
[4] J. Saadoune, C. Delmas, J. Solid State Chem. 136 (1998) 8.
[5] A.G. Ritchie, C.O. Gowa, J.C. Lee, P. Bowles, A. Gilmour, J. Allen, D.A. Rice, F. Brady, S.C.E. Tsang, J. Power Sources 80 (1999) 98.
[6] D. Caurant, N. Baffler, B. Carcia, J.P. Pereira-Ramos, Solid State Ionics 91 (1996) 45.
[7] T. Ohzuku, Y. Makimura, Chem. Lett. 8 (2001) 744.
[8] G. Prado, A. Rougier, L. Fournes, C. Delmas, J. Electrochem. Soc. 147 (2000) 2880.
[9] Y. Sato, T. Kyoano, M. Mukai, K. Kobayakama, Denki Kagaku 66 (1998) 1215.
[10] PNGV Battery Test Manual, Revision 2, DOE/ID-10597, August 1999.
[11] H. Tukamoto, A.R. West, J. Electrochem. Soc. 144 (1997) 3164.
[12] J. Cho, B. Park, J. Power Sources 92 (2001) 35.
[13] S. Liu, K. Fung, Y. Hon, M. Hon, J. Solid State Chem. 167 (2002) 97.
[14] C. Han, J. Yoon, W. Cho, H. Jang, J. Power Sources 136 (2004) 132.
[15] R. Stoyanova, E. Zhecheva, E. Kuzmanova, R. Alcantara, P. Lavela, J.L. Tirado, Solid State Ionics 128 (2000) 1.